

Article

A Dynamic Spectrum Allocation Algorithm for a Maritime Cognitive Radio Communication System Based on a Queuing Model

Jingbo Zhang ¹ , Jianyu Yang ^{1,*}, Yiyang Zhang ² and Shufang Zhang ¹

¹ Information Science and Technology College, Dalian Maritime University, Dalian 116026, China; zhang_jingbo@dlnu.edu.cn (J.Z.); sfzhang@dlnu.edu.cn (S.Z.)

² China Transport Telecommunications & Information Center, Beijing 100011, China; zyy@cttic.cn

* Correspondence: jy_yang@dlnu.edu.cn; Tel.: +86-0411-8472-3118

Received: 23 August 2017; Accepted: 26 September 2017; Published: 27 September 2017

Abstract: With the rapid development of maritime digital communication, the demand for spectrum resources is increasing, and building a maritime cognitive radio communication system is an effective solution. In this paper, the problem of how to effectively allocate the spectrum for secondary users (SUs) with different priorities in a maritime cognitive radio communication system is studied. According to the characteristics of a maritime cognitive radio and existing research about cognitive radio systems, this paper establishes a centralized maritime cognitive radio communication model and creates a simplified queuing model with two queues for the communication model. In the view of the behaviors of SUs and primary users (PUs), we propose a dynamic spectrum allocation (DSA) algorithm based on the system status, and analyze it with a two-dimensional Markov chain. Simulation results show that, when different types of SUs have similar arrival rates, the algorithm can vary the priority factor according to the change of users' status in the system, so as to adjust the channel allocation, decreasing system congestion. The improvement of the algorithm is about 7%–26%, and the specific improvement is negatively correlated with the SU arrival rate.

Keywords: maritime cognitive radio communication system; spectrum allocation algorithm; queuing model with two queues; priority factor; two-dimensional Markov chain

1. Introduction

With the rapid development of wireless technology, spectrum resources have become increasingly scarce resources, thus promoting the rapid development of cognitive radio technology [1–5].

Spectrum sensing and spectrum allocation are important components of cognitive radio. Moreover, spectrum allocation as a key part of cognitive radio technology, has received a great deal of attention from experts and scholars. Cognitive radio spectrum allocation can be divided into two categories according to the network structure [1,6]: centralized spectrum allocation [7–9] and distributed spectrum allocation [10–12]. The two methods of allocation are applied in different networks due to their respective characteristics. Due to primary users' opportunistic access in cognitive radio networks, the ON/OFF model is widely used to represent the status of the channel [13–15]. In a centralized cognitive radio network, secondary users (SUs) choose to wait while primary users (PUs) use channels. If there is no idle channel, SUs will wait for the response of the central base station (CBS). Based on this queuing feature, a great deal of research has been proposed to analyze the cognitive radio system using queuing theory and Markov chains. In [16], a queuing access scheme based on system cost for when SUs has several priorities was proposed. In [17], the author derived system throughput and packet delay, and analyzed a dynamic spectrum access scheme by a Markov chain. In [18], Chu et al. proposed a strategy to coordinate the dynamic spectrum access of different

types of traffic and modeled the state transitions of the dynamic spectrum allocation (DSA) as a multi-dimensional Markov chain. In [19], Wang et al. investigated a two-dimensional birth-and-death process with priority in the cognitive radio system, and a one-dimensional queuing model was derived to equalize the complicated process. In [20], two queuing schemes with novel queue scheduling algorithms, which can assign different priority levels to different traffic types, were proposed, and the priority factor was also introduced to control channel allocation.

With the development of communication technology, the demand for maritime digital communication is increasing. Current maritime wireless communication uses a licensed VHF band or satellite communication to satisfy the requirements of the International Maritime Organization (IMO) [21]. However, IMO requires a wideband and low-cost communication system; the existing system needs to improve maritime services and reduce the communication cost [22]. Several studies regarding maritime communication systems have been done as an attempt to handle the problems of existing systems [22–24]. However, it has been difficult to find spectra to satisfy the demand of high-speed maritime communications. Lack of spectrum resources and low efficiency of fixed spectrum allocation promote the development of maritime cognitive radio. Zhou et al. first proposed the concept of cognitive maritime wireless networks and presented a cognition-enhanced mesh medium access control (MAC) protocol for the operation of the proposed cognitive maritime mesh/ad hoc networks [25]. Ejaz et al. proposed an optimal entropy-based cooperative spectrum sensing in maritime cognitive radio networks [26]. Tang et al. presented a solution to overcome this spectrum scarcity issue by utilizing cognitive radio (CR) technology in the maritime Automatic Identification System (AIS) VHF network [27]. Capela et al. designed a cognitive layer stack and established the idea of software-defined maritime cognitive radio [28].

Compared with cognitive radio on land, maritime cognitive radio has several differences:

- Communications take place on ships, and the CBS is responsible for resource allocation and does not need to participate in data transmission.
- Maritime cognitive radio has unique services, such as position reporting, early warning information, chart updates, meteorological information, and so on. Services that involve navigational safety generally have higher priority levels. The packet lengths of different services are quite different. High-priority services usually have much smaller packets to ensure the efficiency of communication.
- The nodes that are used as CBSs depend on the usage scenario. As the ships are located near the coast, a shore station can be used. Alternatively, as the ships are navigating offshore, at sea, a buoy station should be used [27,29].

Dynamic spectrum allocation is based on the fact that not all users are active at the same time; it is a method that allows users to use the channel when the channel is idle [30,31]. At present, the common spectrum allocation models and algorithms rarely involve the communication between SUs, and discussions of the priority of SUs according to the service type are still few. Therefore, it is necessary to study the dynamic spectrum allocation algorithm of a maritime cognitive radio communication system.

This paper proposes a DSA algorithm for a maritime cognitive radio communication system. In brief, the contributions of this paper can be summarized as follows:

1. Based on the characteristics of maritime cognitive radio, a communication model of the centralized maritime cognitive radio communication system is proposed;
2. According to the communication model, a queuing model that contains two queues and multiple servers is established. The pre-classifier is set to divide the SUs into two queues due to the maritime service type. A two-dimensional Markov chain is used to analyze the queuing model; and
3. A DSA algorithm with priority factor is proposed. The priority factor is decided by the maritime service. Simulation results show that the algorithm can significantly decrease system congestion.

The rest of the paper is organized as follows: In Section 2, we introduce the maritime cognitive radio communication model. In Section 3, a queuing model based on the communication model is presented and a DSA algorithm is proposed. In Section 4, we use a two-dimensional Markov chain to analyze the queuing model and provide the steady-state probability of each state. Section 5 discusses the simulation results of our proposed algorithm. Finally, the paper is concluded in Section 6.

2. Maritime Cognitive Radio Communication Model

2.1. Centralized Cognitive Radio Communication System

With the development of communication technology, the demand for digital communication among ships is increasing. Cognitive radios have been proposed as a solution to overcome spectrum congestion enabling opportunistic use of underutilized bands occupied by licensed users, which is typically the case of the VHF maritime band [22,28]. Therefore, constructing a maritime cognitive radio communication system is of great significance for improving the utilization of spectrum resources.

In cognitive radio, in order to solve the problem of the lack of spectrum resources and low efficiency of fixed spectrum allocation, it is necessary to improve the spectrum utilization and improve the efficiency of system communication, both of which are closely linked with spectrum allocation. Cognitive radio spectrum allocation can be divided into two categories according to the network structure: centralized spectrum allocation and distributed spectrum allocation [17]. Centralized spectrum allocation refers to the existence of a CBS in the network cell, and the CBS completes the spectrum allocation of each user in the cell; furthermore, the distributed spectrum allocation refers to non-CBS: users coordinate with each other to complete the spectrum allocation. Compared with distributed spectrum allocation, centralized spectrum allocation has certain advantages, such as convenient network management, less delay, and the easy control of interference to the PU's network. In view of the maritime wireless communication scenario, the purpose is to realize the data interaction between ship and ship, or between ship and shore station. It is a typical point-to-point direct communication.

As shown in Figure 1, the CBS is a buoy when communications between ships happen at sea, while the shore station is the CBS when the location is close to shore. PU represents licensed users that are authorized to use the VHF maritime band, for example, VHF walkie-talkies and AIS. SU represents the cognitive radio communication equipment installed on the ships which can opportunistically use spectrum. SUs can communicate with each other and the CBS sends control information and receives status information from SUs [1,32].

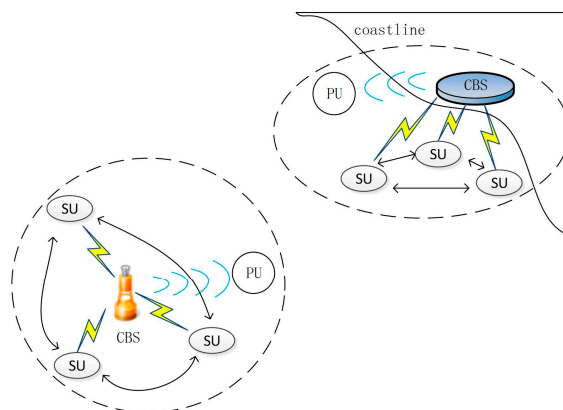


Figure 1. Centralized maritime cognitive radio communication system.

The CBS manages the spectrum resources and allocates channels to SU. At the same time, it is responsible for perceiving the arrival of PUs and notifying SUs to avoid the PUs.

Independently of the ship’s location, the cognitive radio networks evidence the clear characteristics of a centralized cognitive network. Thus, it requires a centralized cognitive radio communications system.

2.2. Design of Service Flow for SUs and CBS

In the maritime cognitive radio communication system, the demand of communication is different depending on the service. Therefore, in the CBS, it is necessary to classify the communication requests according to service type. The CBS needs to make different responses to different types of requests. When the PU uses the channel, it does not need to notify the CBS. This requires that the CBS needs to have the ability to perceive whether a PU is using the channel. If a PU and an SU use the channel at the same time, the CBS must inform the SU to suspend the current communication.

As shown in Figure 2, when an SU makes a communication request, it will send a request packet that contains the SU’s information to the CBS. The CBS receives the request, makes a decision, and then informs the SU of which channel the SU is allowed to use. After receiving the information from the CBS, the SU sends back status information, indicating that the SU is beginning to use the channel. When the SU has finished the communication, status information will also be sent to the CBS to indicate that the channel is not being used anymore. The CBS periodically senses the status information of SUs; the time period during which this occurs is called the sensing period.

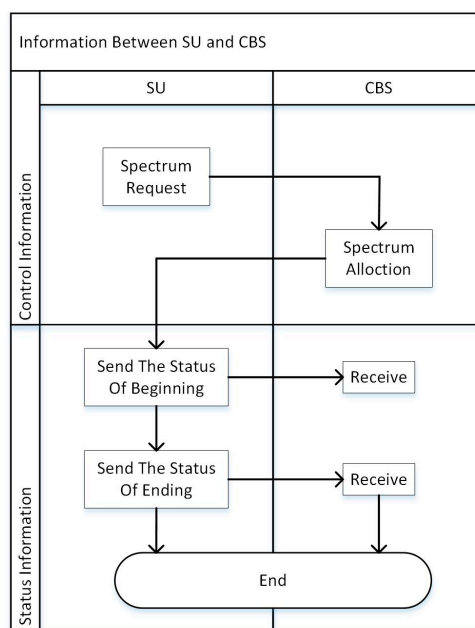


Figure 2. Schematic diagram of the data interaction between the secondary user (SU) and the central base station (CBS).

3. Queuing Model and Dynamic Spectrum Algorithm

In a land communication system, the priorities of SUs are always decided by the data rate requirement of the service and the high real-time requirement of the services [30], while in maritime communication systems, the priorities lie in whether the service is about navigational safety. Services such as position reports and early warning information must have higher priorities than general services, which are not related to navigational safety. To differentiate whether the services involve the information of navigational safety, the CBS divides the communication requests of SUs into a high-priority request queue SU_{q1} and a low-priority request queue SU_{q2} . Based on the two queues with different priorities, we introduce the idea of queuing theory and construct a regional spectrum allocation algorithm based on a queuing model with two queues and multiple servers.

3.1. Queuing Model with Two Queues and Multiple Servers

In recent years, under the auspices of the IMO, the research on e-navigation is in ascendance [33–35]. E-navigation is a system concentrated on information transmission, providing a standard for the data package. Some data bits are used in the package to indicate the type of service, which is called the message ID. In the queuing model, a pre-classifier is used to analyze the type of service by the message ID in the data package. As shown in Figure 3, the SUs' communication requests are divided into queue SU_{q1} and queue SU_{q2} by the pre-classifier. The first arriving request will get the allocation of the CBS first. After assignment, the CBS will inform the SU of some related information. At the same time, the CBS also checks if a PU is using the required channel.

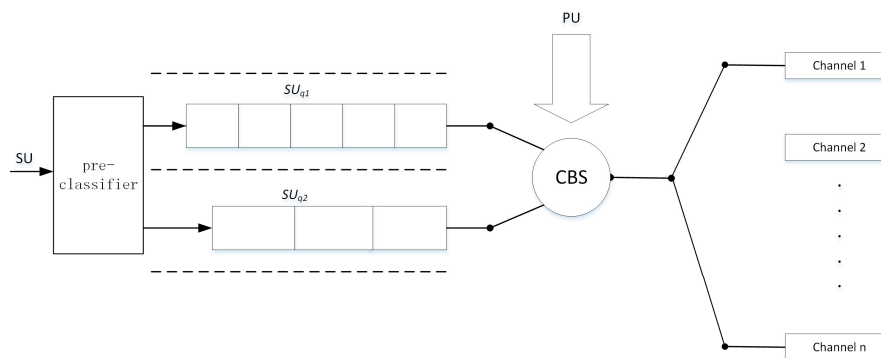


Figure 3. Queuing model with two queues and multiple servers.

As the arrival of each SU's communication request is a random event, the arrival of SUs' communication requests will follow the Poisson distribution [17,36–38]. After the pre-classifier processing, the arrival rate λ_{q1} of the high-priority queue and the arrival rate λ_{q2} of the low-priority queue are also subject to the Poisson distribution.

A large number of papers [17,19,36,37,39] use the exponential distribution as the distribution of the channel service time, which is the time during which SUs use the channel to communicate with each other. Assuming that the service time of SU_{q1} and SU_{q2} follow the exponential distribution with parameters μ_{q1} and μ_{q2} , the average service rates of the two queues will equal μ_{q1} and μ_{q2} , respectively.

Since the use of the channel by a PU is also a random process of continuous time, its arrival rate follows the Poisson distribution with parameter λ_p , and its service time follows the exponential distribution with a mean of μ_p^{-1} [17,19,20].

In order to ensure the communication efficiency of the high-priority queue, we introduce the adaptive priority parameter p in the DSA algorithm to dynamically adjust the weight of the two request queues.

3.2. SU State Transitions

Since there are two types of queues at CBS, the channel state of the cognitive radio communication system with N channels can be described by an integer pair (i, j) , where i represents the number of channels occupied by SU_{q1} , j represents the number of channels occupied by SU_{q2} .

When an SU of SU_{q1} arrives with rate λ_{q1} , the state of the system becomes $(i + 1, j)$. Similarly, when an SU of SU_{q2} arrives with rate λ_{q2} , the state of the system becomes $(i, j + 1)$. At the state (i, j) , when an SU in SU_{q1} leaves with rate $i\mu_{q1}$, the state of the system becomes $(i - 1, j)$; when an SU in SU_{q2} leaves with rate $j\mu_{q2}$, the state of the system becomes $(i, j - 1)$. Furthermore, when $i + j = N$, SU_{q2} enters the blocking state. The CBS will determine whether SU_{q1} preempts the channel of SU_{q2} according to priority factor p , which characterizes the probability that SU_{q2} will refuse to stop using channels. Thus, when the CBS determines that SU_{q1} preempts SU_{q2} 's channel, the system state changes from $(N - i, i)$ to $(N - i + 1, i - 1)$, and the state transition rate is λ_i , which is given as

$$\lambda_i = (1 - p^i)\lambda_{q1}. \tag{1}$$

3.3. Impact of PU

In a cognitive radio communication system, SUs must vacate channels when a PU uses the channel. This section discusses SUs that are insensitive to delay, which means that SUs choose to wait when encountering the PU’s intervention and continue to transmit after the PU is finished.

Since SUs must give up the channel when a PU is attempting to use it, the service time originally obeying a certain distribution will change due to the intervention of the PU.

The status of the channel occupied by the PU can be divided into busy and idle [17,18,40,41]; thus, the state transition diagram of the PU can be drawn—1 means busy, 0 means idle—as Figure 4 shows.

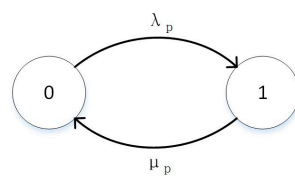


Figure 4. State transition diagram of the primary user (PU).

Considering that the sum of all steady state probabilities is 1, a PU’s busy probability P_B and PU’s idle probability P_I are given as

$$P_B = \frac{\lambda_p}{\lambda_p + \mu_p} \tag{2}$$

$$P_I = \frac{\mu_p}{\lambda_p + \mu_p}. \tag{3}$$

Let C be the service time of the SU under the PU’s intervention and let T be the service time of the SU without the PU’s intervention. N_d represents the number of PUs appear during the service time of the SU. D_r represents the service time remaining when the SU is interrupted by the PU. The letter s is the complex variable in the Laplace transform. We then obtain

$$C = T + \sum_{r=1}^{N_d} D_r \tag{4}$$

$$\begin{aligned} E[e^{-sC} | T, N_d] &= e^{-sT} E[\exp(-s \sum_{r=1}^{N_d} D_r)] \\ &= e^{-sT} \left(\frac{\mu_p}{s + \mu_p}\right)^{N_d}. \end{aligned} \tag{5}$$

Through the total probability theorem, we obtain

$$E[C] = -\frac{E[e^{-sC}]}{ds} \Big|_{s=0}. \tag{6}$$

In [19], the author discussed the case when the PU was involved. According to the Laplace transform of the service time distribution of the SU when the SU is under the PU’s interference, the author obtained the average service time via statistical theory, and proved that an equivalent service time distribution is consistent with the negative exponential distribution when they have equal expectation. Let μ_q be the average service rate of SU:

$$\mu_q = \frac{1}{E[C]}. \tag{7}$$

Therefore, considering the two kinds of SUs with different priorities and the existence of a PU, let μ_{q1}' and μ_{q2}' be the average service rates of SU_{q1} and SU_{q2} . We thus obtain

$$\mu_{q1}' = \mu_{q1}P_I \tag{8}$$

$$\mu_{q2}' = \mu_{q2}P_I. \tag{9}$$

3.4. Blocking Coefficient

When the total number of channels occupied by SUs in a cognitive radio communication system is N , the assignable channels of the CBS reaches a maximum. The newly arriving requests of SU_{q2} cannot receive a response from the CBS so that leading to enter the blocking state. The newly arriving request of SU_{q1} obeys the allocation of the CBS, and data transmission continues if SU_{q1} receives the channel of SU_{q2} ; if not, a blocking state is reached.

The steady state probability of the system state (i, j) is donated as $P_{i,j}$. The blocking probabilities of SU_{q1} and SU_{q2} are represented by S_{s1} and S_{s2} , respectively. S_{s1} and S_{s2} are given by

$$S_{s1} = P_{N,0} + \sum_{i=0}^{N-1} P_{i,N-i} p^{N-i} \tag{10}$$

$$S_{s2} = \sum_{i=0}^N P_{i,N-i}. \tag{11}$$

Because only SU_{q1} and SU_{q2} exist in the system, the system blocking coefficient S is defined as

$$S = S_{s1} + S_{s2}. \tag{12}$$

3.5. Dynamic Spectrum Allocation Algorithm

The change of arrival rates of SU and PU can change the usage of the channel. Correspondingly, the CBS should also change the priority factor p so as to reduce the system blocking coefficient by changing the allocation of the channels.

The CBS first senses whether there is a PU. If the PU occupies the channel, it informs all SUs to stop using the channel. If not, then it determines whether there is an idle channel. If there is an idle channel, a fixed priority factor is used to directly respond to the SU's request and the CBS assigns the channel. When an idle channel does not exist, the CBS evaluates the status of the channel occupied by SU_{q1} and SU_{q2} in a sensing period, so as to adjust the channel allocation by changing the priority factor p .

After a sensing period, if the SU's arrival rate and status of the channel do not change, the CBS does not change the priority factor; if one of them changes in the next sensing period, the CBS adjusts the priority factor p to reduce the blocking coefficient of the system.

When the arrival rates of SU_{q1} and SU_{q2} vary, the system congestion will inevitably change. The algorithm optimizes the system blocking coefficient by changing the priority factor p , which depends on the numbers of different SUs in the system. It is easy to write the average number of SU_{q1} and SU_{q2} . If E_{s1} and E_{s2} are the average numbers of SU_{q1} and SU_{q2} , then we obtain

$$E_{s1} = \sum_{i=0}^N \sum_{j=0}^{N-i} iP_{i,j} \tag{13}$$

$$E_{s2} = \sum_{i=0}^N \sum_{j=0}^{N-i} jP_{i,j}. \tag{14}$$

When there are more users of SU_{q1} in the system, there should be a greater probability of preempting SU_{q2} 's channel. We obtain

$$1 - p = E_{s1} / (E_{s1} + E_{s2}) \tag{15}$$

$$p = E_{s2} / (E_{s1} + E_{s2}). \tag{16}$$

The CBS adjusts the priority factor p to realize the dynamic allocation of the spectrum according to the condition of the system. Algorithm 1 is the DSA algorithm.

Algorithm 1: Dynamic Spectrum Allocation Algorithm

```

1  if PU occupy the Channel
2  Tell SU stop using the channel
3  else if Any channel idle
4  Allocate channels to  $SU_{q1}$  &  $SU_{q2}$ 
5  else
6  do
7  Evaluate the status of users in system
8  Adjust the priority factor  $p$ 
9  While (Arrival rates of SU change)
10 Adjust the channels allocation Of  $SU_{q1}$  &  $SU_{q2}$ 
11 end

```

4. Markov Chain Analysis

In Section 3.2, the state transition of the SU was analyzed. The state of the channel is divided into busy and idle only; meanwhile, the system has two kinds of SUs and the integer pair (i, j) can indicate the state of the channels occupied by SUs. A user will obtain the channel or join in the queue when it arrives, while a user will leave the system when it completes communication. In a cognitive radio communication system, arrival is random and the occupancy of channels is memory-less. The arrival and leaving of users constitutes a birth-and-death process, so we use a Markov chain to analyze the model [19,42].

The property of Markov chain is denoted as

$$P\{X_{n+1} = j | X_n = i, X_{n-1} = i_{n-1}, \dots, X_1 = i_1, X_0 = i_0\} = P\{X_{n+1} = j | X_n = i\}. \tag{17}$$

The state of the system is only related to the previous state in the Markov chain. A one-dimensional Markov chain has only one class of states, while a two-dimensional Markov chain has two classes. Due to the state transition of the system, we can draw the state transition diagram of the two-dimensional Markov chain, as shown in Figure 5.

Since the number of one class of states is N , there are $(N + 1) \times (N + 2) / 2$ states in the system, the steady state probability of state (i, j) is represented by $P_{i,j}$. According to the state transition diagram, the steady state equations for each state are listed:

State $(0, 0)$:

$$P_{0,0}(\lambda_{q1} + \lambda_{q2}) = P_{1,0}\mu_{q1} + P_{0,1}\mu_{q2}. \tag{18}$$

State $(i, 0)$, where $1 \leq i \leq N - 1$:

$$P_{i,0}(\lambda_{q1} + \lambda_{q2} + i\mu_{q1}) = P_{i+1,0}(i + 1)\mu_{q1} + P_{i,1}\mu_{q2} + P_{i-1,0}\lambda_{q1}. \tag{19}$$

State $(0, j)$, where $1 \leq j \leq N - 1$:

$$P_{0,j}(\lambda_{q1} + \lambda_{q2} + j\mu_{q2}) = P_{1,j}\mu_{q1} + P_{0,j+1}(j + 1)\mu_{q2} + P_{0,j+1}\lambda_{q2}. \tag{20}$$

State (i, j) , where $1 \leq i \leq N - 2, 1 \leq j \leq N - i - 1$:

$$P_{i,j}(i\mu_{q1} + j\mu_{q2} + \lambda_{q1} + \lambda_{q2}) = P_{i+1,j}(i+1)\mu_{q1} + P_{i,j+1}(j+1)\mu_{q2} + P_{i-1,j}\lambda_{q1} + P_{i,j-1}\lambda_{q2} \quad (21)$$

State $(i, N - i)$, where $1 \leq i \leq N - 1$:

$$P_{i,N-i}[i\mu_{q1} + (N - i)\mu_{q2} + \lambda N - i] = P_{i-1,N-i}\lambda_{q1} + P_{i,N-i-1}\lambda_{q2} + P_{i-1,N-i+1}\lambda_{N-i+1} \quad (22)$$

State $(0, N)$:

$$P_{0,N}(N\mu_{q2} + \lambda N) = P_{0,N-1}\lambda_{q2} \quad (23)$$

State $(N, 0)$:

$$P_{N,0}N\mu_{q1} = P_{N-1,0}\lambda_{q1} + P_{N-1,1} + \lambda_1 \quad (24)$$

The sum of the steady state probabilities of all states in system is 1, so

$$\sum_{j=0}^N \sum_{i=0}^{N-j} P_{i,j} = 1 \quad (25)$$

From Equations (18)–(25), we can calculate the steady-state probabilities of all states, changing the equations into a matrix.

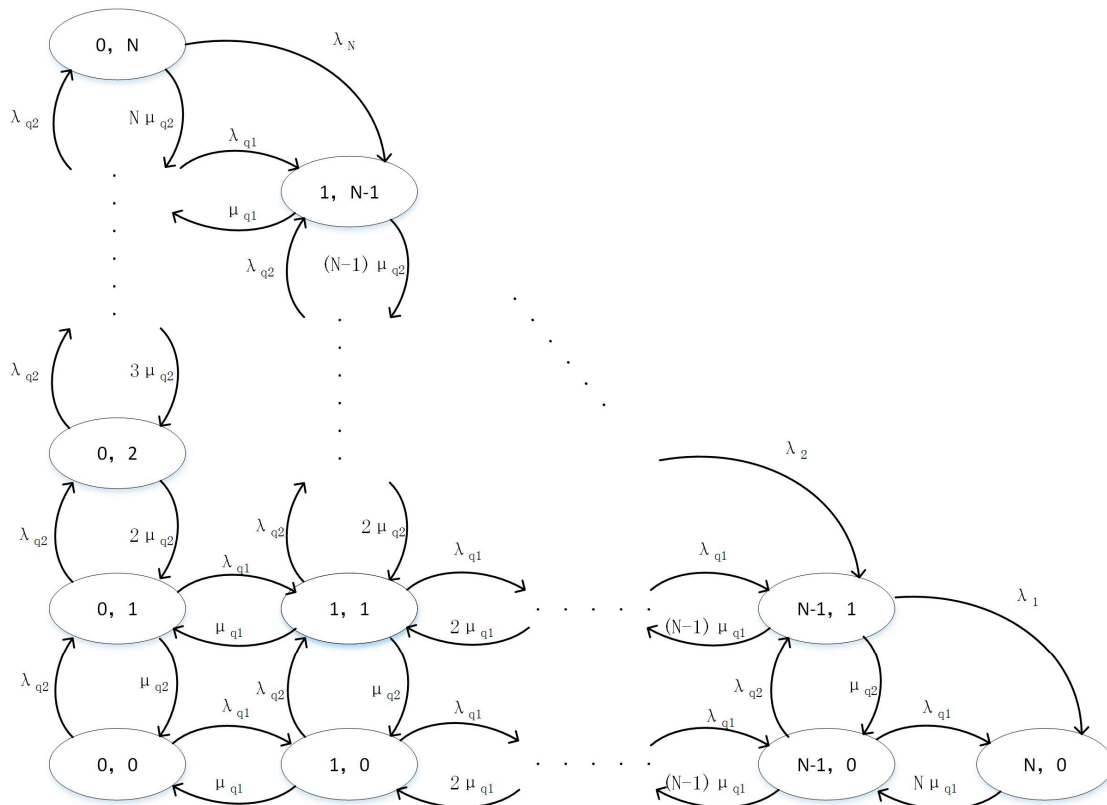


Figure 5. State transition diagram of the two-dimensional Markov chain.

Column vector A is the steady state probabilities of all states, and A is given as

$$A = (P_{0,0}, P_{0,1}, \dots, P_{0,N}, P_{1,0}, \dots, P_{1,N-1}, \dots, P_{i,j}, \dots, P_{N-1,1}, P_{N,0})^T \quad (26)$$

Matrix M is the coefficient matrix of the steady-state equations:

$$M = (m_1, m_2, \dots, m_{(N+1)(N+2)/2}, m_{(N+1)(N+2)/2+1})^T. \tag{27}$$

Among the matrix M , m_i ($1 \leq i \leq (N + 1)(N + 2)/2$) is the coefficient row vector of the steady-state equation of state i in vector A , and $m_{(N+1)(N+2)/2+1}$ is a row vector of 1.

B is a column vector, the number of 0 in the column vector is $(N + 1)(N + 2)/2$:

$$B = (\underbrace{0, 0, 0, \dots, 0}_{(N+1)(N+2)/2}, 1). \tag{28}$$

From Equations (22)–(24), we obtain

$$MA = B. \tag{29}$$

According to Equation (25), the steady-state probabilities of each state can be given as

$$A = M^{-1}B. \tag{30}$$

5. Simulation and Analysis

MATLAB (from MathWorks, Natick, MA, USA) was used to analyze the reduction of the blocking coefficient by the DSA algorithm. The service rate represents the speed of the SU using the channel, so it is negatively correlated with the size of the packet. In order to ensure the efficiency of its communication, the length of packets in the high-priority queue are usually much smaller than those in the low-priority queue. The simulation is carried out with the parameters set as follows:

- Set the service rate of high priority request queue $\mu_{q1} = 2$;
- Set the service rate of low priority request queue $\mu_{q2} = 0.2$;
- Set the number of channels controlled by CBS $N = 3$;
- Set the arrival rate of PU $\lambda_p = 1$; and
- Set the service rate of PU $\mu_p = 1$.

We analyze the relationship between the priority factor p and the arrival rates λ_{q1} and λ_{q2} . After 10,000 random simulations, we obtain the results shown in Figure 6. The red dots represent the value of the priority factor p as λ_{q1} and λ_{q2} vary. We mark the points in blue when the difference between λ_{q1} and λ_{q2} is below 5%. From Figure 6, under a 98% probability condition, the value of the priority factor p corresponding to the blue mark point is within the range of 0.2–0.8.

Then we analyze the relationship between the average number of users in the system and the arrival rate of the users' requests in both queues. We set λ_{q1} and λ_{q2} to increase from 0 to 5 in steps of 0.02 and obtain the average number of users by 62,500 points. Figure 7 depicts the average number of users in the system as λ_{q1} and λ_{q2} vary. With the arrival rate of SU changing, the upper bound of the average number of users does not exceed the number of system channels N .

The DSA algorithm adjusts the priority factor p according to the change of the average number of users in the system. To simplify the analysis, let SU_{q1} 's arrival rate λ_{q1} be an independent variable and the arrival rate of SU_{q2} is set as $\lambda_{q2} = 1$. We make λ_{q1} increasing from 0 to 5 in steps of 0.005. Figure 8 depicts the variation of the average numbers of SU_{q1} , SU_{q2} , and total users in the system as λ_{q1} varies.

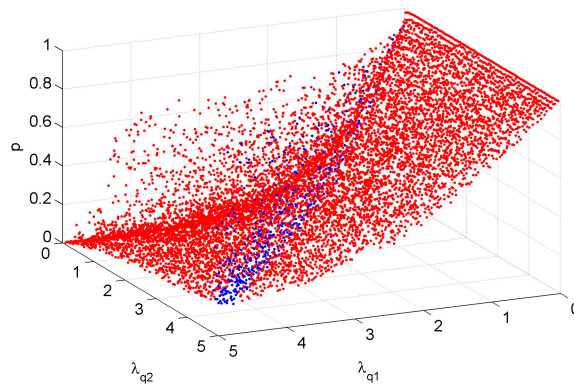


Figure 6. The range of p when λ_{q1} and λ_{q2} are similar.

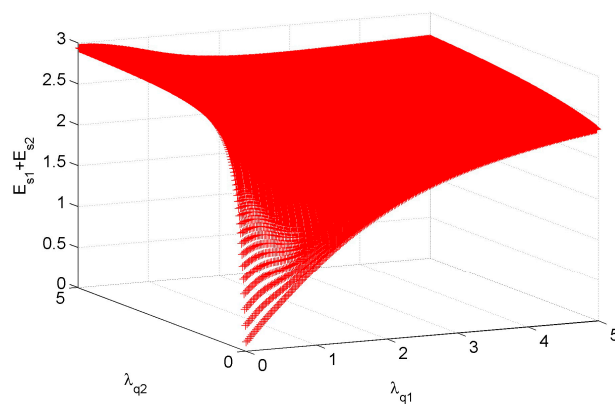


Figure 7. Average number of users as λ_{q1} and λ_{q2} vary.

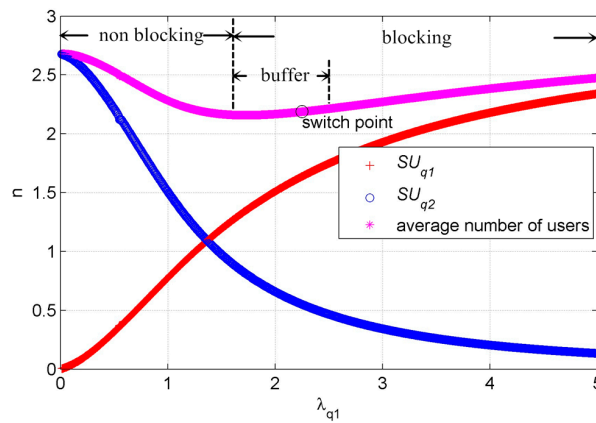


Figure 8. Average numbers of SU_{q1} , SU_{q2} , and total users.

With the increase of λ_{q1} , the average number of SU_{q1} increases, the average number of SU_{q2} decreases, and the average number of total users in the system first decreases and then increases. This is because when λ_{q1} is small enough, only the communication requests in the low-priority queue occupy the system; however, with the increase of λ_{q1} , the channels are shared by SU_{q1} and SU_{q2} , so the system does not appear in a blocking state. As a result, the average number of total users shows a downward trend. However, as λ_{q1} continues to increase, the average number of total users also continues to increase, and the system appears to be in a blocking state. According to the system status, the DSA algorithm will switch the fixed priority factor to the dynamic priority factor, and the dynamic priority factor is further adjusted according to the status change of the system.

In [20], the author proposed the idea that the priority factor is determined according to the system status and requirements, but the implementation is not discussed. Instead, a fixed priority factor is determined according to the initial status of the users. The author analyzed the model with a priority factor $p = 1/3$.

In order to prevent the wrong switch of the priority factor, we set a buffer in which CBS selects the switching point. The buffer allows the switch point to be within the 2% error range of the minimum average number of total users. Our analysis is with respect to a switching point of $\lambda_{q1} = 2.25$.

Figure 8 shows the judge of the state and the choice of the switch point. Based on this, we set λ_{q1} as increasing from μ_{q1}' to 5 by steps of 0.005. Figure 9 compares the blocking coefficients when we use different fixed priority factors and the DSA algorithm as λ_{q1} varies. We observe that, when λ_{q1} is slightly larger than μ_{q1}' , the system does not appear to be in a blocking state, and when the algorithm uses the fixed priority factor $p = 0.2$, the blocking coefficient is smaller than other values of p ; after the switch point, the algorithm changes to use the dynamic priority factor, and the blocking coefficient is also smaller than other values of p . It can be proved that the DSA algorithm proposed in this paper can reduce the blocking coefficient of the system.

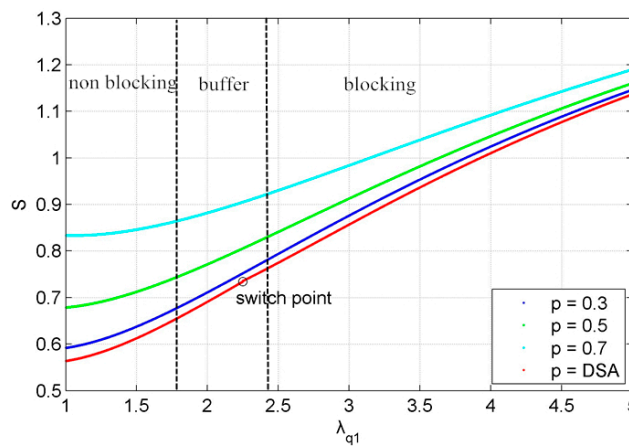


Figure 9. The blocking coefficient of the dynamic spectrum allocation (DSA) algorithm and fixed priority factors.

Figure 10 shows the improvement of system congestion coefficient by the DSA algorithm as p and λ_{q1} vary. According to the conclusion of Figure 6, the range of parameter p is 0.2–0.8. The value of the arrival rate λ_{q1} is 2.25–5. Figure 9 shows that the system is in a blocked state, and the DSA algorithm adaptively adjusts the priority factor.

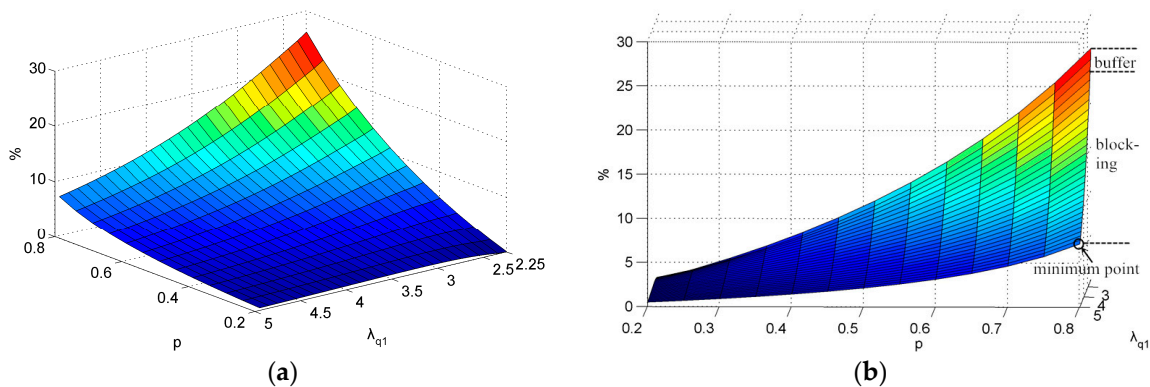


Figure 10. Improvement of the system congestion coefficient. (a) Three-dimensional perspective; (b) Side view.

When using the fixed priority factor, we can obtain the congestion coefficients of system S . While using the adaptively priority factor, we can obtain S' . The improvement of the system's congestion coefficient means $(S' - S)/S$. In Figure 10b, we can see an improvement when the system is at the blocking state. The improvement is positively related to the size of the fixed priority factor and negatively related to the arrival rates of SU_{q1} . When the parameter p is 0.8, we can obtain the minimum point in Figure 10b, so that the improvement of the algorithm corresponding to the lowest point tends to 7%. This means that, as the arrival rate λ_{q1} increases, the improvement of the algorithm will decrease, but the minimum still has about 7% improvement. The vertex of the graph indicates the maximum degree which the DSA algorithm can reduce when λ_{q1} is near the switch point.

Finally, we can determine that the DSA algorithm, with an adaptive adjustment of the priority factor, can effectively improve the system efficiency. The improvement of the algorithm is about 7–26%, and the specific improvement value is negatively correlated with the SU arrival rate.

6. Conclusions

The rapid development of maritime digital communication leads to a growing demand for spectrum resources. Maritime cognitive radio receives more and more attention, as it can utilize the inefficient limited spectrum resources.

Considering the current available research about the common cognitive radio and the characteristics of maritime cognitive radio, we established a centralized maritime cognitive radio communication model. The model sets up signal channels for the CBS to control the data transmission in the system, which embodies the characteristics of maritime wireless communications.

Based on the model, we create a simplified queuing model with two queues with priority. We analyze the system model by using a two-dimensional Markov chain. A DSA algorithm, which achieves the channel allocation for SUs with different priorities, is proposed. The algorithm adjusts the channel allocation by the priority factor according to the system status. Simulation results show that, when different kinds of SUs have similar arrival rates, the improvement is positively related to the size of the fixed priority factor and negatively related to the arrival rates of SU_{q1} . Additionally, the DSA algorithm, with an adaptive adjustment of the priority factor, can effectively improve system efficiency. The improvement of the algorithm is about 7%–26% and the specific improvement is negatively correlated with the SU arrival rate.

Acknowledgments: This work was supported by the Chinese National Science Foundation under grants 61501078 and 61231006, and the Fundamental Research Funds for the Central Universities under grants 3132016208.

Author Contributions: Jingbo Zhang designed the maritime cognitive radio communication system model, the dynamic spectrum allocation algorithm based on a queuing model, and organized the paper; Jianyu Yang was responsible for writing and editing the manuscript and conducted the simulation work; Yiyang Zhang and Shufang Zhang supervised the work and contributed to the writing of the paper.

Conflicts of Interest: The authors declare no conflict of interest.

References

1. Wang, B.; Liu, K.J.R. Advances in cognitive radio networks: A survey. *IEEE J. Sel. Top. Signal Process.* **2011**, *5*, 5–23. [[CrossRef](#)]
2. Ding, G.; Wu, Q.; Yao, Y.D.; Wang, J.; Chen, Y. Kernel-Based Learning for Statistical Signal Processing in Cognitive Radio Networks: Theoretical Foundations, Example Applications, and Future Directions. *IEEE Signal Process. Mag.* **2013**, *30*, 126–136. [[CrossRef](#)]
3. Mitola, J.; Maguire, G.Q. Cognitive radio: Making software radios more personal. *IEEE Pers. Commun.* **1999**, *6*, 13–18. [[CrossRef](#)]
4. Haykin, S. Cognitive radio: Brain-empowered wireless communications. *IEEE J. Sel. Areas Commun.* **2005**, *23*, 201–220. [[CrossRef](#)]
5. Yucek, T.; Arslan, H. A survey of spectrum sensing algorithms for cognitive radio applications. *IEEE Commun. Surv. Tutor.* **2009**, *11*, 116–130. [[CrossRef](#)]

6. Yu, J.; Konaka, S.; Akutagawa, W.; Zhang, Q.Y. Cross-Entropy-Based Energy-Efficient Radio Resource Management in HetNets with Coordinated Multiple Points. *Information* **2016**, *7*, 3. [[CrossRef](#)]
7. Chen, Z.; Gao, F. Cooperative-Generalized-Sensing-Based Spectrum Sharing Approach for Centralized Cognitive Radio Networks. *IEEE Trans. Veh. Technol.* **2016**, *65*, 3760–3764. [[CrossRef](#)]
8. Sharifi, M.; Sharifi, A.; Niya, M.J.M. A new weighted energy detection scheme for centralized cognitive radio networks. In Proceedings of the 7th International Symposium on Telecommunications (IST), Tehran, Iran, 9–11 September 2014; pp. 1004–1008. [[CrossRef](#)]
9. Mastorakis, G.; Mavromoustakis, C.X.; Bourdena, A.; Kormentzas, G.; Pallis, E. Maximizing energy conservation in a centralized cognitive radio network architecture. In Proceedings of the 18th International Workshop on Computer Aided Modeling and Design of Communication Links and Networks (CAMAD), Berlin, Germany, 25–27 September 2013; pp. 175–179. [[CrossRef](#)]
10. Parzy, M.; Bogucka, H. Distributed spectrum allocation with the Cournot competition. In Proceedings of the 18th European Signal Processing Conference, Aalborg, Denmark, 23–27 August 2010; pp. 1454–1458.
11. Zubow, A.; Doering, M.; Wolisz, A. Distributed Spectrum Allocation for Autonomous Cognitive Radio Networks. In Proceedings of the 20th European Wireless Conference on European Wireless, Barcelona, Spain, 14–16 May 2014; pp. 1–7.
12. Derakhshani, M.; Le-Ngoc, T. Distributed Learning-Based Spectrum Allocation with Noisy Observations in Cognitive Radio Networks. *IEEE Trans. Veh. Technol.* **2014**, *63*, 3715–3725. [[CrossRef](#)]
13. Zhang, R. On peak versus average interference power constraints for protecting primary users in cognitive radio networks. *IEEE Trans. Wirel. Commun.* **2009**, *8*, 2112–2120. [[CrossRef](#)]
14. Jiang, C.; Chen, Y.; Liu, K.J.R.; Ren, Y. Renewal-theoretical dynamic spectrum access in cognitive radio network with unknown primary behavior. *IEEE J. Sel. Areas Commun.* **2013**, *31*, 406–416. [[CrossRef](#)]
15. Jiang, T.; Wang, H.; Vasilakos, A.V. QoE-Driven Channel Allocation Schemes for Multimedia Transmission of Priority-Based Secondary Users over Cognitive Radio Networks. *IEEE J. Sel. Areas Commun.* **2012**, *30*, 1215–1224. [[CrossRef](#)]
16. Xu, R.S.; Jiang, T. A Cost Based Bubble-Queuing Access Scheme in Multi-Priority Cognitive Radio Network. *Acta Electron. Sin.* **2014**, *42*, 1147–1156. [[CrossRef](#)]
17. Tumuluru, V.K.; Wang, P.; Niyato, D.; Song, W. Performance Analysis of Cognitive Radio Spectrum Access with Prioritized Traffic. *IEEE Trans. Veh. Technol.* **2012**, *61*, 1895–1906. [[CrossRef](#)]
18. Chu, T.M.C.; Zepernick, H.J.; Phan, H. Channel reservation for dynamic spectrum access of cognitive radio networks with prioritized traffic. In Proceedings of the International Conference on Communication Workshop (ICCW), London, UK, 8–12 June 2015; pp. 883–888. [[CrossRef](#)]
19. Wang, L.; Peng, Q.Z.; Peng, Q.H. Reward Based Multichannel Step-queuing Access Scheme in Cognitive Radio. *J. Electron. Inf. Technol.* **2012**, *34*, 1944–1949. [[CrossRef](#)]
20. Balapuwaduge, I.A.M.; Jiao, L.; Pla, V.; Li, F.Y. Channel Assembling with Priority-Based Queues in Cognitive Radio Networks: Strategies and Performance Evaluation. *IEEE Trans. Wirel. Commun.* **2014**, *13*, 630–645. [[CrossRef](#)]
21. Zhou, M.-T.; Hoang, V.D.; Harada, H.; Pathmasuntharam, J.S.; Wang, H.; Kong, P.-Y.; Ang, C.-W.; Ge, Y.; Wen, S. TRITON: High-speed maritime wireless mesh network. *IEEE Wirel. Commun.* **2013**, *20*, 134–142. [[CrossRef](#)]
22. Ejaz, W.; Hasan, N.U.; Shah, G.A.; Kim, H.S.; Anpalagan, A. Biologically Inspired Cooperative Spectrum Sensing Scheme for Maritime Cognitive Radio Networks. *IEEE Syst. J.* **2017**. [[CrossRef](#)]
23. Lambrinos, L.; Djouvas, C. Creating a maritime wireless mesh infrastructure for real-time applications. In Proceedings of the GLOBECOM Workshops (GC Wkshps), Houston, TX, USA, 5–9 December 2011; pp. 529–532. [[CrossRef](#)]
24. Mu, L. A hybrid network for maritime on-board communications. In Proceedings of the 8th International Conference on Wireless and Mobile Computing, Networking and Communications (WiMob), Barcelona, Spain, 8–10 October 2012; pp. 761–768. [[CrossRef](#)]
25. Zhou, M.T.; Harada, H. Cognitive maritime wireless mesh/ad hoc networks. *J. Netw. Comput. Appl.* **2012**, *35*, 518–526. [[CrossRef](#)]
26. Ejaz, W.; Shah, G.A.; Hasan, N.; Kim, H.S. Optimal Entropy-Based Cooperative Spectrum Sensing for Maritime Cognitive Radio Networks. *Entropy* **2013**, *15*, 4003–5011. [[CrossRef](#)]

27. Tang, C.; Kandeepan, S.; Hourani, A.; Munari, A.; Berioli, M. Spectrum sensing for cognitive maritime VHF networks. In Proceedings of the OCEANS 2014-TAIPEI, Taipei, Taiwan, 7–10 April 2014; pp. 1–7. [[CrossRef](#)]
28. Capela, G.; Rodrigues, A.; Sanguino, J.E.; Bolas, E. Opportunistic usage of the maritime VHF band using a software defined cognitive radio. In Proceedings of the 1st URSI Atlantic Radio Science Conference (URSI AT-RASC), Las Palmas, Spain, 16–24 May 2015. [[CrossRef](#)]
29. Singh, D.; Kimbahune, S.; Singh, V.V. Mobile signal extension in deep sea—Towards a safe and sustainable fisheries. In Proceedings of the ITU Kaleidoscope: ICTs for a Sustainable World (ITU WT), Bangkok, Thailand, 14–16 November 2016; pp. 1–8. [[CrossRef](#)]
30. Yang, S.H.; Wang, J.K.; Han, Y.H.; Jiang, X.L. Dynamic spectrum allocation algorithm based on matching scheme for smart grid communication network. In Proceedings of the 2nd IEEE International Conference on Computer and Communications (ICCC), Chengdu, China, 14–17 October 2016; pp. 3015–3019. [[CrossRef](#)]
31. Nissel, R.; Rupp, M. Dynamic spectrum allocation in cognitive radio: Throughput calculations. In Proceedings of the International Black Sea Conference on Communications and Networking (BlackSeaCom), Varna, Bulgaria, 6–9 June 2016; pp. 1–5. [[CrossRef](#)]
32. Chen, T.; Zhang, H.; Maggio, G.M.; Chlamtac, I. Topology Management in CogMesh: A Cluster-Based Cognitive Radio Mesh Network. In Proceedings of the International Conference on Communications, Glasgow, UK, 24–28 June 2007; pp. 6516–6521. [[CrossRef](#)]
33. Wozniak, J.; Gierlowski, K.; Hoefl, M. Broadband communication solutions for maritime ITSs: Wider and faster deployment of new e-navigation services. In Proceedings of the 15th International Conference on ITS Telecommunications (ITST), Warsaw, Poland, 29–31 May 2017; pp. 1–11. [[CrossRef](#)]
34. Park, D.; Lee, K.; Park, S. Common Vocabulary Set for Support of Interoperability of Data Contents of Maritime Equipment and Systems in E-Navigation Services. In Proceedings of the 6th International Conference on IT Convergence and Security (ICITCS), Prague, Czech Republic, 26 September 2016; pp. 1–4. [[CrossRef](#)]
35. Oh, S.H.; Seo, D.; Lee, B.; Chung, B. Mutual Authentication between Ships in the E-Navigation Environment. In Proceedings of the 7th International Conference on Security Technology, Haikou, China, 20–23 December 2014; pp. 15–18. [[CrossRef](#)]
36. Filippini, I.; Cesana, M.; Malanchini, I. Competitive spectrum sharing in cognitive radio networks: A queuing theory based analysis. In Proceedings of the First International Black Sea Conference on Communications and Networking (BlackSeaCom), Batumi, Georgia, 3–5 July 2013; pp. 238–242. [[CrossRef](#)]
37. Chouhan, L.; Trivedi, A. Priority based MAC scheme for cognitive radio network: A queuing theory modelling. In Proceedings of the Ninth International Conference on Wireless and Optical Communications Networks (WOCN), Indore, India, 20–22 September 2012; pp. 1–5. [[CrossRef](#)]
38. Dudin, A.N.; Lee, M.H.; Dudina, O.; Lee, S.K. Analysis of Priority Retrial Queue With Many Types of Customers and Servers Reservation as a Model of Cognitive Radio System. *IEEE Trans. Commun.* **2017**, *65*, 186–199. [[CrossRef](#)]
39. Zhang, M.; Wei, G.; He, C.X.; Wang, H.J. Performance of Cognitive Radio Network with Different Packet Level Policy. *J. South China Univ. Technol.* **2010**, *38*, 101–105. [[CrossRef](#)]
40. Msumba, J.A.; Xu, H. Throughput optimization MAC scheme for cognitive radio networks: A POMDP framework. In Proceedings of the Africon, Pointe-Aux-Piments, Mauritius, 9–12 September 2013; pp. 1–5. [[CrossRef](#)]
41. Oluwaranti, A.; Okegbile, S. Two state Markov chain based predictive model for cognitive Radio spectrum availability: A conceptual approach. In Proceedings of the Future Technologies Conference (FTC), San Francisco, CA, USA, 6–7 December 2016; pp. 179–186. [[CrossRef](#)]
42. El-Toukhey, A.T.; Ammar, A.A.; Tantawy, M.M.; Tarrad, I.F. Performance analysis of different opportunistic access based on secondary users priority using licensed channels in Cognitive radio networks. In Proceedings of the 34th National Radio Science Conference (NRSC), Alexandria, Egypt, 13–16 March 2017; pp. 160–169. [[CrossRef](#)]

